Fabrication, structural and adsorption studies of zirconium oxide nanoparticles

*Ayman A. Ali, Sayed A. Shama, Sahar R. EL-Sayed**
Chemistry Dept., Faculty of Science, Benha Univ., Benha, Egypt
E-Mail: sahar.rashad@fsc.bu.edu.eg

Abstract

The current research presents the fabrication of zirconium oxide by using a precipitation method followed by calcination at 400 ^{o}C for 2 h. The calcined powder was confirmed by different tools such as X-ray diffraction (XRD), Fourier transform infrared spectra (FT-IR), Field emission scanning electron microscope (FE-SEM) and transmission electron microscope (TEM). The XRD results revealed that the average crystallite size of the fabricated zirconium oxide nanoparticles was 5 nm. FTIR spectra showed the peak at 450 cm^{-1} corresponding to the crystalline ZrO_2 nanoparticles. The effect of contact time, initial dye concentration, adsorbent dosage and pH was studied. The adsorption data fitted the pseudo-first-order kinetic model. The adsorption followed Langmuir adsorption isotherm model compared to the freundlich isotherm model. Thermodynamic parameters for the adsorption system were showed that the adsorption process is spontaneous, physiorption and endothermic. The prepared product has efficient adsorption performance to naphthol green B dye (NGB) with a maximum adsorption capacity of 51.54 $mg.g^{-1}$.

Keywords: Zirconium oxide nanoparticles, precipitation method, Adsorption; structural, Naphthol green B dye.

1. Introduction

Water pollution is one of the major global problems in our modern civilization which leads to the deaths of people daily [1]. Recent years, environmental contaminations have a significant attention to introduce the various solutions for removal a wide class of pollutants from wastewater. Out of all the contaminants exist in industrial fields, organic dyes are a significant kind of pollutants [2]. Dyes are colored organic compounds based on two main functional groups such as chromophoric group (NR_2, NHR, NH_2, COOH and OH), and auxochromes (N_2, NO and NO_2) [3] which lead to increasing the organic pollutants inside the water media. Dyes are widely utilized in different fields such as food processing, textile or leather manufacturing, rubber and plastics industry, paper printing, cosmetics or medicine industry [4]. Inorganic and organic pollutants are existed inside the environment area such as heavy metal and dyes which considered the big problems as result of their carcinogenic and toxic characteristics for living things in our planet. The trace amount of the dye exist in the living systems may cause several health problems to mankind as well as animals [5].

Naphthol Green B dye is a derivative of benzidine and napthoic acid and metabolizes to carcinogenic products. It may affect blood factors, such as induce somnolence and clotting, and respiratory problems [5]. Removing colour from waste water can be done via several methods namely chemical, biological and physical methods such as flocculation, adsorption, oxidation, electrolysis, biodegradation, ion-exchange, photo catalysis, coagulation, ozonation membrane filtration and etc. Among the various available physical–chemical processes, adsorption is considered as one of the most effective and confirmed method for decolorization in water and effluent [6].

Nanocomposites with organic and inorganic nano-fillers have attracted immense interest from different fields because of the unbeatable characteristics of nanoparticles such as high surface reactivity, large surface area and relatively low cost [7-11]. Among the various available materials, Zirconium oxide with chemical formula ZrO_2, occasionally known as zirconia is a white crystalline oxide of zirconium [12]. ZrO_2 exhibits three important polymorphic forms: the monoclinic phase is thermodynamically stable up to 1100 ^{o}C, the tetragonal phase exists in the temperature range 1100-2370 ^{o}C, and the cubic phase is found above 2370 ^{o}C [13]. Zirconium oxide is a widely used inorganic material which is chemically stable, non-toxic, and soluble in water [14], and is of vital importance due to its thermal and chemical stability, and excellent mechanical properties, such as high strength and fracture toughness, high melting point, low thermal conductivity, and high corrosion resistance [15]. ZrO_2 nanostructures materials illustrate intriguing much attention of researchers due to their unique physical, chemical, optical, and electrical and applications in different areas such as photocatalysis, sensing, coatings, wastewater treatment, fuel cells, advanced ceramics and catalysis [16].

In this study, ZrO_2 nanoparticles were fabricated by precipitation method. The synthesized zirconium oxide characterized using different techniques. The prepared nanoparticles were used as adsorbent for the adsorption and removal of NGB from aqueous solution. The kinetics, thermodynamic and adsorption isotherm of NGB were also studied.

2. Experimental

2.1. Materials and reagents

Zirconium oxychloride octahydrate ($ZrOCl_2.8H_2O$, 99.5%), and naphthol green B dye

($C_{30}H_{15}FeN_3Na_3O_{15}S_3$, 99%) were purchased from Sigma–Aldrich Chemical Company. Nitric acid (HNO_3, 69%) and ammonium hydroxide (NH_4OH, 33%) were purchased from El Nasr pharmaceutical chemical company. The initial pH was adjusted with NaOH or HCl solutions. All chemicals and reagents were of analytical grade and used as received without any purification. Freshly bidistilled water was used through all experiments. The structure of naphthol green B dye is shown in Figure 1.

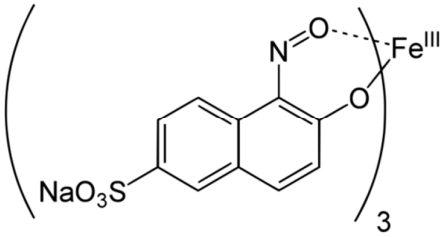

Figure 1. The chemical structure of NGB dye.

2.2. Fabrication of zirconium oxide nanoparticles (ZONP) via precipitation method

Zirconium oxychloride octahydrate (3.22 g, 0.01 mol) was dissolved in 20 mL bidistilled water and heated on hotplate with magnetic stirring at 60 ^oC for 5 min. Zirconium ions precipitated from cold solution by drop wise addition of NH_4OH solution until pH =9. The obtained precipitate was washed for several times and dried at 150 ^oC for overnight, producing a white powder. The as-prepared powder was calcined at 400 ^oC for 2h to get the pure crystalline ZrO_2 nanoparticles (ZONP).

2.3. Characterization

The crystallinity and phase purity of the as-prepared nanomaterials were identified by using x-ray powder diffraction, 18 KW diffractometer (Bruker; model D 8 advance) with monochromatic Cu-Ka radiation, 1.54178 (A^o) at room temperature in the angular range of 10^o-80^o (2Θ) with step size 0.02^o (2Θ) and scan step time 0.4 (s). The as-prepared samples were measured using FTIR spectrometer (Thermo Scientific; model Nicolet iS10) at room temperature from 4000 to 400 cm^{-1}. The morphology and particle size of the as-prepared products were studied using HR-TEM (model Tecnai G20, FEI, Netherland) at an electron voltage of 200 KV. The morphology and elemental composition of the as-prepared nanomaterials were investigated using Field emission scanning electron microscope (SEM, JEOL JSM-6390) joined with energy dispersive x-ray spectroscopy (EDS, Oxford Instruments, Model No: 7582) operating at an accelerating voltage of 20 KV. The (FE-SEM) and gold coating process by using EMITECH K550X sputter coater. The adsorption studies were investigated by using a Jasco UV-Vis spectrophotometer (Jasco; model V 670).

2.4. Batch adsorption studies

Adsorption properties of the prepared nanoparticles were investigated by studying different adsorption conditions such as pH, contact time, initial concentrations, adsorbent dose and temperature. Dye solutions were fabricated by dissolving the dye under study in deionized water to get the required concentrations. Uptake values were determined using the measured and initial dye concentrations. The data obtained in batch mode studies was used to calculate the adsorption capacity (q_e) and the removal efficiency (%R) from equation No. 1 and 2, respectively.

$$q_e = \frac{(C_o - C_e)V}{m} \quad (1)$$

$$\text{Removal (R\%)} = \frac{(C_o - C_e)}{C_o} \times 100 \quad (2)$$

Where, q_e is the amount of dye molecules adsorbed per unit weight of adsorbent (mg g^{-1}), V is the volume of solution (L), C_o is the initial dye concentration (mg/L), C_e is the equilibrium dye concentration (mg/L), and m is the weight of the adsorbent (g).

3. Results and discussion

3.1. X-ray studies

Figure 2(i) shows XRD pattern of the obtained product (ZONP) sample and the peaks match well with the zirconium oxide nanoparticles according to XRD card no. 01-079-1771 (space group P42/nmc; a=3.5916 Å, b= 3.5916 Å, c= 5.179 Å and $\alpha = \beta = \gamma = 90^o$). The crystallite sizes of the calcined ZONP sample were calculated by using the Debye-Scherrer formula [17] (equation No. 3). The average crystallite size (D) of the obtained ZrO_2 was determined to be 5 nm.

$$D = 0.9\lambda/\beta \cos\theta \quad (3)$$

Where, λ is the wavelength of X-ray (1.5406 A for Cu Kα), θ is the Bragg diffraction angle and β is the x-ray full width of the diffraction peak at half-maximum height.

3.2. FTIR studies

Figure 2(ii) displays FTIR spectrum of the annealed ZONP sample. The vibrational bands appeared at ca. 3250 cm^{-1} and 1610 cm^{-1} are corresponding to vibrational spectrum modes of the adsorbed water molecules on the surface of zirconium oxide nanoparticles. FTIR spectrum of the calcined ZONP sample showed a band at 450 cm^{-1} related to the crystalline ZrO_2 nanoparticles [16, 18-22].

3.3. The morphology studies

The particle size and morphology of obtained zirconium oxide ZONP sample are investigated by

FE-SEM and HR-TEM. The FE-SEM images of the calcined ZrO_2 nanoparticles using precipitation method and after calcination at 400 ^oC are represented in Figure 2(iii). Images reveal the presence of ultrafine and crystalline spherical and non-spherical shapes with agglomeration. The average grain size of the calcined ZrO_2 (ZONP sample) was determined from SEM images and it was found to be 50 nm. The determined size was larger than that calculated from XRD pattern, indicated that the appearance of the collection of the fine particles with each other as densification. Figure 2(iv) displays HR-TEM micrograph of the calcined ZONP sample. The TEM micrograph showed a spherical shape with agglomeration and the average particle sizes were about 15 nm. From the extracted XRD, SEM and TEM data, the presence of the soft collection and densification particles with each other were obvious.

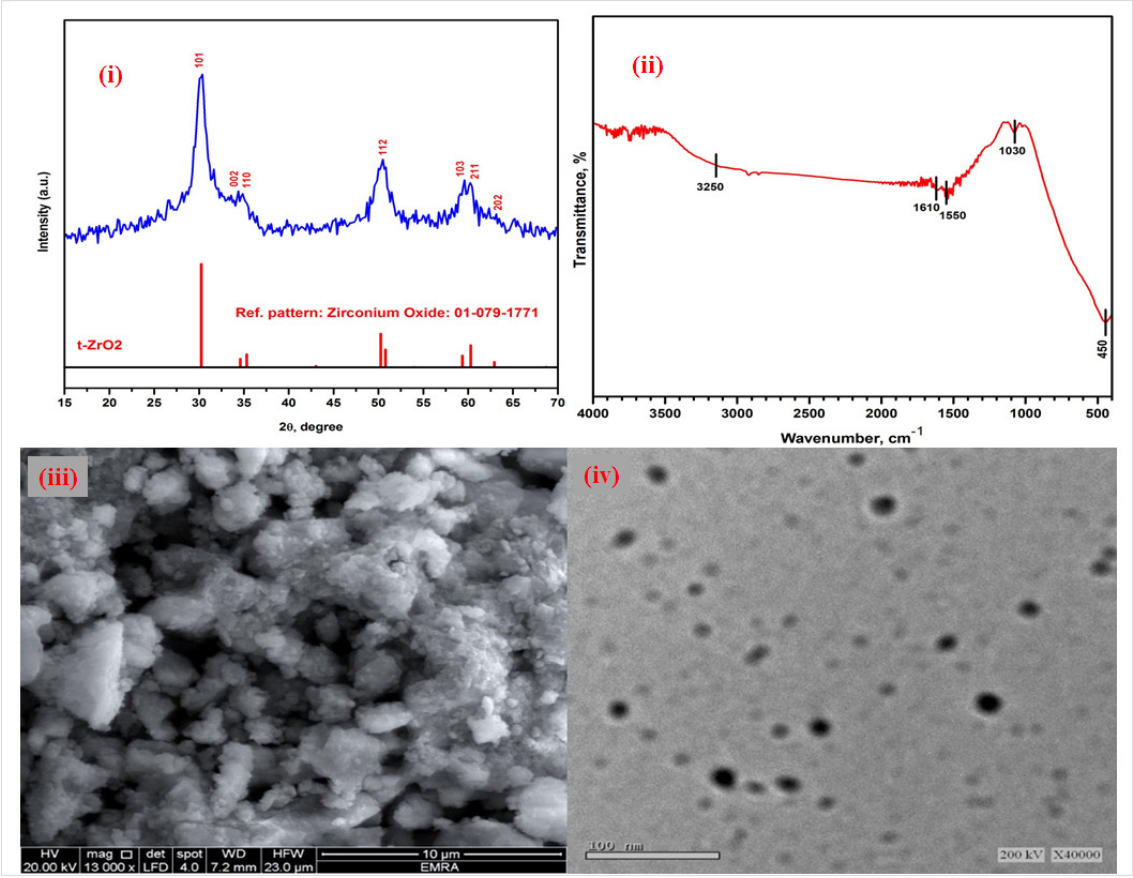

Figure 2. XRD pattern (i), FTIR spectrum (ii), FE-SEM image (iii) and HR-TEM image (iv) of the obtained zirconium oxide (ZONP sample) after calcination at 400 ^oC.

3.4. Adsorption studies

3.4.1 Effect of pH

Figure 3(i) shows the effect of initial pH (3 to 9) on the adsorption of 50 mg/L of NBG dye solution over 50 mg of ZONP sample. The removal efficiency recorded downward trend by increasing the pH values. The removal dye efficiency recorded at λ_{max} =714 nm and it reached its maximum value (98.5%) at pH = 3.

3.4.2 Effect of contact time

The contact time of the removal 50 mg/L of NGB was tested using 50 mg of ZONP sample at pH 3. Figure 3(ii) displays the removal efficiencies for the NGB over ZONP sample as a function of contact times ranging between 15 and 240 min. The rate of uptake was rapid in the beginning and become gradual in the later stages until it reached a saturation state. The maximum removal of NGB dye was attained in 120 min to be 24.63 mg/g.

3.4.3 Effect of initial concentration

Figure 3(iii) shows the effect of various initial concentrations for the removal of NGB dye over ZONP sample with 0.05 g of ZrO_2 at pH=3. After 120 min, the adsorption capacities were determined from the extracted data. The rate of uptake was rapid in the beginning and reached saturation as result of the maximum availability of

active sites on the surface of the ZONP sample. As the time passed, the active sites were blocked, the rate of the separation of dye decreased.

3.4.4 Effect of adsorbent dose

The effect of ZrO_2 quantity on the removal 50 mg/L of NGB dye was investigated by adding various amounts (0.01–0.125 g) of ZONP sample as adsorbent and the pH of the solutions were fixed at 3. After 120 min, the efficiencies were calculated and presented in Figure 3(iv). The extracted data indicated that the increasing adsorbent dosage lead to increasing the removal of NGB dye on ZONP material due to the rising the number of the active centers of the as-prepared ZONP sample.

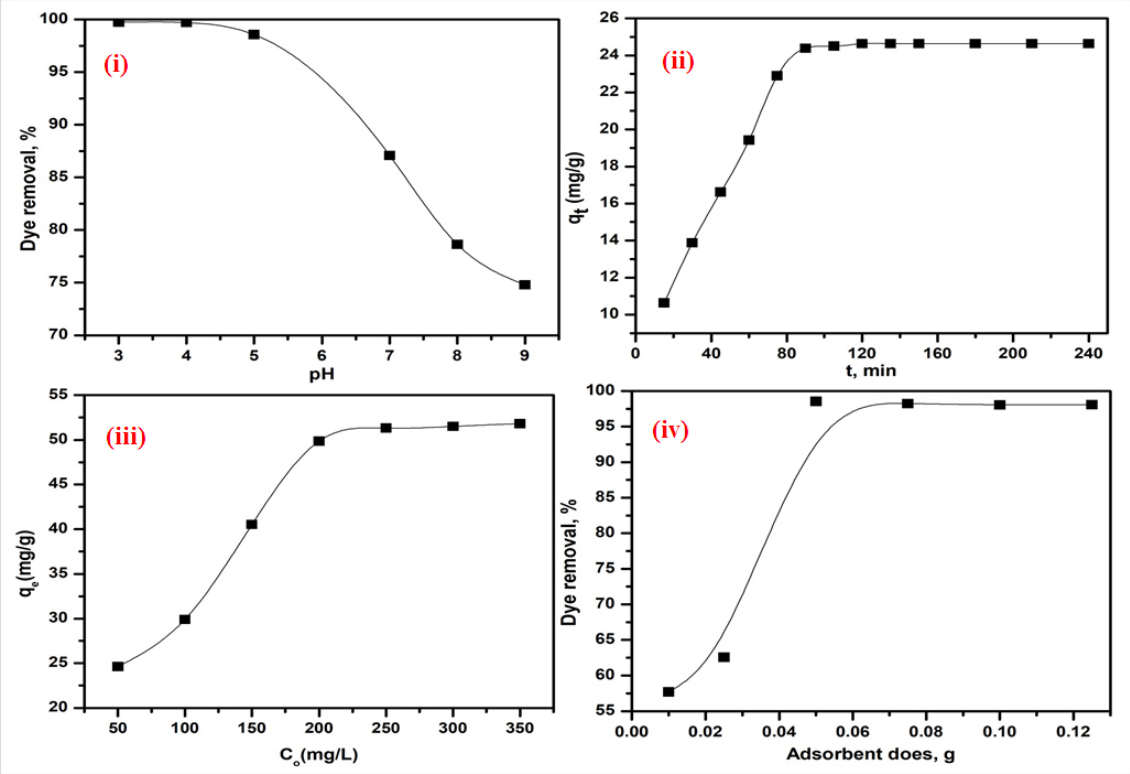

Figure 3. Influence of pH (i), time (ii), initial concentration (iii) and adsorbent dose (iv) on the removal of the NGB dye over the ZONP nanoparticle.

3.5. Adsorption isotherms studies

The adsorption isotherms models were carried out by studying the relation of the adsorption capacities with the various initial concentrations of the dye (50-350 mg/L). The maximum value of the adsorption capacity was found 51.54 mg/g. Langmuir and Freundlich isotherm models are utilized for the description of the experimental data using different equilibrium concentrations of NGB dye (50-350 mg/L) over 0.05 gram of ZrO_2 sample at pH=3 and 303 K. Linear plots of Langmuir [23-25] (C_e/q_e with C_e) and Freundlich [26, 27] ($\ln q_e$ with $\ln C_e$) isotherm models are displayed in Figure 4(a and b) according to the equations No. 4 and 5, respectively.

$$\frac{C_e}{q_e} = \frac{1}{K_L q_m} + \frac{C_e}{q_m} \qquad (4)$$

$$\ln q_e = \ln K_F + \frac{1}{n} \ln C_e \qquad (5)$$

Where, C_e is the equilibrium concentration of NGB dye in solution (mg/L), q_e is the equilibrium adsorption capacity of NGB dye on ZrO_2 adsorbent, K_L is the Langmuir parameter (L/mg), q_m is the maximum quantity of adsorbed solute to adsorbent (mg/g), K_f is the freundlich constant (mg/g) and (1/n) is the heterogeneity factor.

From Langmuir isotherm, the equilibrium parameter can be calculated from $R_L=1/(1+K_L C_o)$; where, the values of R_L reflects the nature of the adsorption process (if the values of R_L in between 0-1, the adsorption process is favorable). From Freundlich isotherm, the maximum adsorption capacity can be calculated using the relation: $q_m = K_f C_o^{1/n}$. Besides if value of (1/n) <1, it indicates a normal adsorption. In addition to, the value of n in

between 1<n<10, indicates a favorable adsorption process [28].

Table 1 outlined the factors extracted from Langmuir and Freundlich isotherm. From the R^2 values, Langmuir isotherm model is a better fitting than the Freundlich isotherm. It means that the uptake of the NGB dye over the ZrO_2 nano-adsorbent in the form of a monolayer without any interaction between adsorbed molecules on a homogenous surface [29]. Besides, the estimated adsorption capacity ($q_{m(cal)}$) from the Langmuir isotherm model was determined to be 55.56 mg/g which was closed to the experimental value ($q_{m(exp)}$) (51.54 mg/g). In the current study, R_L values were found to be in the range of 0.0628-0.2509 which was corresponding to the initial concentrations 50-250 mg/g. It reflects that the adsorption of NGB dye over the ZONP sample is a favorable process. The R^2 value of Langmuir equation was found to be 0.9852 and it was closer to 1, compared to the R^2 value obtained from the Freundlich isotherm model.

Table (1) The extracted parameters from Langmuir and Freundlich isotherms for ZrO_2 adsorbent (ZONP sample).

Adsorption isotherm	Parameter	Value
Langmuir parameters	K_L (L/mg)	0.0597
	$q_{m\ (cal)}$ (mg/g)	55.56
	R_L	0.0628-0.2509
	R^2	0.9852
	$q_{m\ (exp)}$ (mg/g)	51.54
Freundlich parameters	K_F [(L/mg) $(L/mg)^{1/n}$]	23.91
	$q_{m\ (cal)}$ (mg/g)	50.77
	n (L/mg)	7.3314
	R^2	0.8069
	$q_{m\ (exp)}$ (mg/g)	51.54

3.6. Adsorption kinetic studies

The adsorption kinetic models were examined by studying the effect of contact time on the separation of NGB dye over ZrO_2 adsorbent. Kinetic factors of the removal NGB dye on ZrO_2 nano-adsorbent were estimated using pseudo-first order equation (plot log (q_e - q_t) against t)[30] and pseudo-second-order equation (plot t/ q_t versus time t)[31] as represented in equations No. 6 and 7. The relations were applied to get some information about the adsorbate quantity and the separation process rate through the calculation of kinetic factors as exhibited in Figure 4(c and d). The calculated data are outlined in Table 2.

$$\log(q_e - q_t) = \log q_e - \frac{k_1}{2.303} \qquad (6)$$

$$\frac{t}{q_t} = \frac{1}{k_2 {q_e}^2} + \frac{t}{q_e} \qquad (7)$$

Where, q_e and q_t are the amounts of dye adsorbed (mg/g) at equilibrium and time t (min), respectively, t (min) is contact time, and k_1 is pseudo-first-order rate constant of adsorption (min^{-1}) and k_2 (g/mg. min) is pseudo- second-order rate adsorption constant. From Table 2 and depending on the R^2 values on 200 mg/L, the pseudo-first-order model is better fitting (r^2= 0.9664) than the pseudo-second-order (r^2= 0.9519) for the removal of the NGB dye over ZrO_2 nano-adsorbent. So, we can say that the removal of NGB dye over ZrO_2 follows the pseudo-first-order model and the calculated adsorption capacity value (cal.51.38 mg/g) is in good agreement with the experimental one (49.85 mg/g).

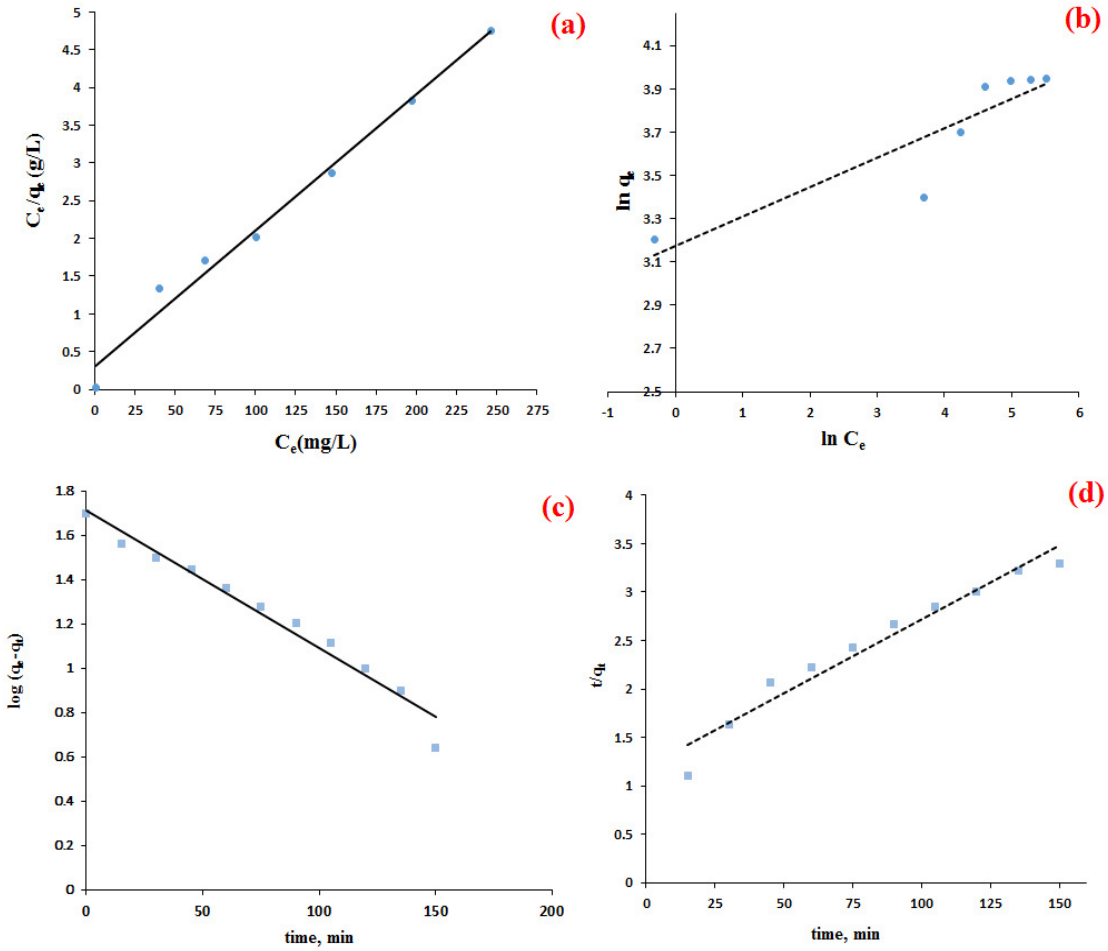

Figure 4. Langmuir (a), Freundlich (b) Pseudo first order model (c) and Pseudo second order model (d) for removal the NGB dye using ZONP sample.

Table (2) Kinetic parameters for the adsorption of NGB dye on ZrO_2 adsorbent.

Kinetic parameters	Parameter	Value
Pseudo first order	$K_1(min^{-1})$	0.0143
	$q_{m\ (cal)}$ (mg/g)	51.38
	R^2	0.9664
	$q_{m\ (exp)}$ (mg/g)	49.85
Pseudo second order	K_2(g/mg.min)	0.0003
	$q_{m\ (cal)}$ (mg/g)	54.7
	R^2	0.9519
	$q_{m\ (exp)}$ (mg/g)	49.85

3.7. Thermodynamic studies

The adsorption process was tested at 303, 308 and 318 k separately for the removal of 50 mg/L of NGB dye using 0.05 g of ZrO_2 nano-adsorbent. The experimental data showed that the adsorption capacity increased slowly with increase in the solution temperature for the separation of NGB dye over ZONP sample as exhibited in Figure 5(a). This indicated that the removal of NGB dye on the synthesized ZrO_2 nano-adsorbents was an endothermic process. The values of thermodynamic factors: ΔH^o, ΔS^o and ΔG^o, were calculated by using van't Hoff equation [32], (equation No. 8) as shown in Figure 5(b).

The values of Gibbs free energy (ΔG^o) for the removal of NGB dye over ZrO_2 nano-adsorbent were calculated from the equation No. 9.

$$\ln K_c = \frac{\Delta S^\circ}{R} - \frac{\Delta H^\circ}{RT} \quad (8)$$

$$\Delta G^\circ = \Delta H^\circ - T\Delta S^\circ \quad (9)$$

Where ΔH^o is enthalpy change, ΔS^o is entropy change, the values of the equilibrium constant (K_c) were determined from q_e/c_e (L/g), T is the temperature in Kevin (k) and R is the gas constant (8.314 J/ mol). Plotting $\ln(k_c)$ against 1/T gives a straight line as represented in Figure 5(b) with a slope ($-\Delta H^o/R$) and a intercept ($\Delta S^o/R$). The calculated thermodynamic constants are outlined in Table 3. The removal of NGB dye using ZrO_2 nano-adsorbent were endothermic process as the value of ΔH^o was positive. The value of ΔH^o (cal. 36.79 KJ/mol) is lower than 40 KJ/mol, therefore the adsorption of NGB dye over ZONP sample is a physisorptive process [5, 33]. ΔS^o has a positive value that means increasing in degree of freedom of solution for separation process. The negative values of ΔG^o revealed that the adsorption process is a spontaneous process. Additionally, the ΔG^o values increased in the negative direction with increasing of temperature that means the removal of NGB dye is more favorable at high temperatures.

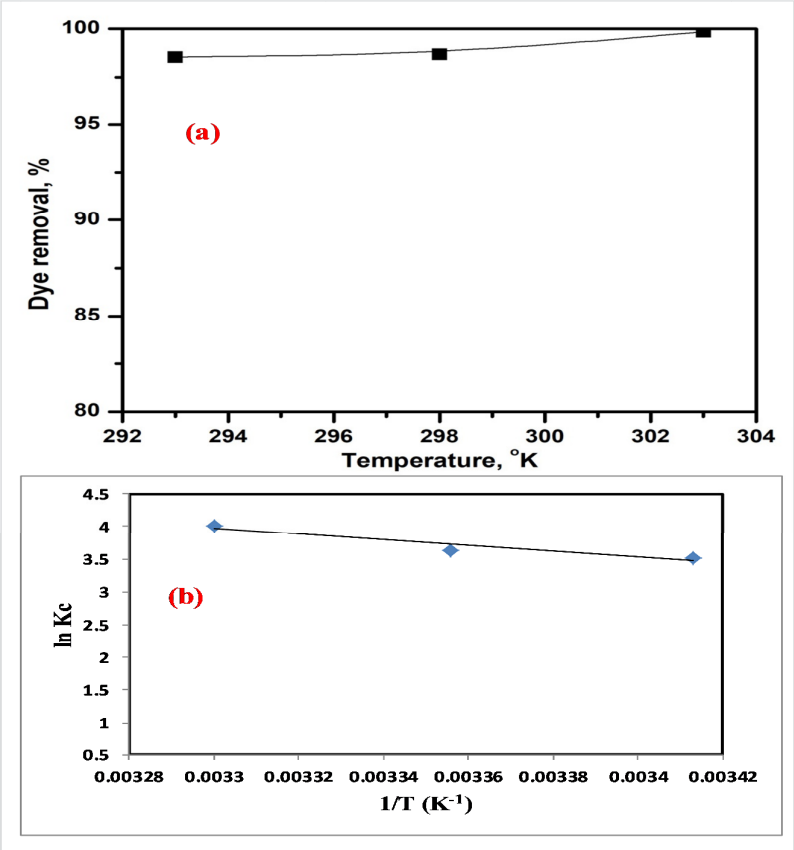

Figure 5. Effect of temperature (a) and Thermodynamic parameters (b) for the adsorption of NGB dye on ZrO2 adsorbent.

Table (3) Thermodynamic parameters for the adsorption of NGB dye on ZrO_2 adsorbent.

Temperature (°K)	ln K_c	ΔG^o (KJ/mol)	ΔH^o (KJ/mol)	ΔS^o (KJ/mol)
293	3.5176	-8.4478	36.79	0.1544
298	3.6202	-9.2197		
303	4.0177	-9.9916		

Conclusions

A precipitation method was utilized for the fabrication of ZrO_2 nanoparticles followed by calcination at 400 ^oC for 2 h. The synthesized product was characterized using various analytical techniques such as scanning electron microscopy (SEM), transmission electron microscope (TEM), X-ray diffraction (XRD) and Fourier transform infrared spectroscopy (FT-IR). ZrO_2 nanoparticles were used as adsorbents for the rapid removal of naphthol green B from the aqueous phase using the batch mode. Adsorption properties of the synthesized product were investigated by studying different adsorption conditions such as contact time, initial dye concentrations, pH, temperature and adsorbent dosage. The adsorption data showed that the adsorption behavior fitted the Langmuir isotherm, and pseudo-first-order models. Thermodynamic parameters for the adsorption system were showed that the adsorption process is spontaneous, physiorption and endothermic.

Acknowledgements

The authors express their thanks to Benha University, Egypt for support of the current research.

References

[1] L. Schell, Modern water: A biocultural approach to water pollution at the Akwesasne Mohawk Nation, Am J Hum Biol., (2019) e23348-e23348.

[2] S. Shakoor, A. Nasar, Removal of methylene blue dye from artificially contaminated water using citrus limetta peel waste as a very low cost adsorbent, J. Taiwan Inst. Chem. Eng., 66 (2016) 154-163.

[3] A. Kausar, M. Iqbal, A. Javed, K. Aftab, H.N. Bhatti, S. Nouren, Dyes adsorption using clay and modified clay: A review, J. Mol. Liq., 256 (2018) 395-407.

[4] L. Bartoňová, L. Ruppenthalová, M. Ritz, Adsorption of Naphthol Green B on unburned carbon: 2-and 3-parameter linear and non-linear equilibrium modelling, Chin. J. Chem. Eng., 25 (2017) 37-44.

[5] M. Attallah, I. Ahmed, M.M. Hamed, Treatment of industrial wastewater containing Congo Red and Naphthol Green B using low-cost adsorbent, Environ. Sci. Pollut. Res., 20 (2013) 1106-1116.

[6] F. Dehghani, S. Hashemian, A. Shibani, Effect of calcination temperature for capability of MFe2O4 (M= Co, Ni and Zn) ferrite spinel for adsorption of bromophenol red, J. Ind. Eng. Chem., 48 (2017) 36-42.

[7] R. Riahi-Madvaar, M.A. Taher, H. Fazelirad, Synthesis and characterization of magnetic halloysite-iron oxide nanocomposite and its application for naphthol green B removal, Appl. Clay Sci., 137 (2017) 101-106.

[8] M. Gabal, F. Al-Solami, Y. Al Angari, A. Ali, A. Al-Juaid, K.-w. Huang, M.J.C.I. Alsabban, Auto-combustion synthesis and characterization of perovskite-type LaFeO3 nanocrystals prepared via different routes, Ceram. Int., 45 (2019) 16530-16539.

[9] A.A. Ali, M.Y. Nassar, A.E.M. El Sharkwy, I.S. Ahmed, M. Abd, E.A. Elhalim, Fabrication and study of Nickel oxide nanoparticles via low combustion synthesis method using different fuels, J. Basic Environ. Sci., 6 (2019) 183-186.

[10] A.A.A. Ahmed, I. S., Sol-gel auto-combustion fabrication and optical properties of cobalt orthosilicate: Utilization as coloring agent in polymer and ceramic, Mater. Chem. Phys., 238 (2019) 121888-121902.

[11] A. Ali, E. El Fadaly, I.S. Ahmed, Near-infrared reflecting blue inorganic nano-pigment based on cobalt aluminate spinel via combustion synthesis method, Dyes Pigm., 158 (2018) 451-462.

[12] B. Sathyaseelan, E. Manikandan, I. Baskaran, K. Senthilnathan, K. Sivakumar, M. Moodley, R. Ladchumananandasivam, M. Maaza, Studies on structural and optical properties of ZrO2 nanopowder for opto-electronic applications, J. Alloys Compd., 694 (2017) 556-559.

[13] M.N. Tahir, L. Gorgishvili, J. Li, T. Gorelik, U. Kolb, L. Nasdala, W. Tremel, Facile synthesis and characterization of monocrystalline cubic ZrO2 nanoparticles, Solid State Sci., 9 (2007) 1105-1109.

[14] H. Cui, Q. Li, S. Gao, J.K. Shang, Strong adsorption of arsenic species by amorphous zirconium oxide nanoparticles, J. Ind. Eng. Chem., 18 (2012) 1418-1427.

[15] L. Li, W. Wang, Synthesis and characterization of monoclinic ZrO2 nanorods by a novel and simple precursor thermal decomposition approach, Solid State Commun., 127 (2003) 639-643.

[16] M. Verma, V. Kumar, A. Katoch, Synthesis of ZrO2 nanoparticles using reactive magnetron sputtering and their structural, morphological and thermal studies, Mater. Chem. Phys., 212 (2018) 268-273.

[17] P. Scherrer, Göttinger Nachrichten Math, Phys, 2 (1918) 98-100.

[18] L. Liang, Y. Xu, D. Wu, Y. Sun, A simple sol–gel route to ZrO2 films with high optical performances, Mater. Chem. Phys., 114 (2009) 252-256.

[19] N. Chandra, D.K. Singh, M. Sharma, R.K. Upadhyay, S. Amritphale, S. Sanghi, Synthesis and characterization of nano-sized zirconia powder synthesized by single emulsion-assisted direct precipitation, J. Colloid Interface Sci., 342 (2010) 327-332.

[20] S. Zinatloo-Ajabshir, M. Salavati-Niasari, Synthesis of pure nanocrystalline ZrO2 via a simple sonochemical-assisted route, J. Ind. Eng. Chem., 20 (2014) 3313-3319.

[21] I.M. Ibrahim, M.E. Moustafa, M.R. Abdelhamid, Effect of organic acids precursors on the morphology and size of ZrO2 nanoparticles for photocatalytic degradation of Orange G dye from aqueous solutions, J. Mol. Liq., 223 (2016) 741-748.
[22] S. Manjunatha, M. Dharmaprakash, Microwave assisted synthesis of cubic Zirconia nanoparticles and study of optical and photoluminescence properties, J. Lumin. 180 (2016) 20-24.
[23] H.P. AkankshaKalra, C. Hui, H. Mackey, T. Ansari, J. Saleem, G. McKay, Adsorption of Dyes from Water on to Bamboo-Based Activated Carbon-Error Analysis Method for Accurate Isotherm Parameter Determination, J. Water Sci. Eng., 1 (2019) 1-11.
[24] S. Rizk, M.M. Hamed, Batch sorption of iron complex dye, naphthol green B, from wastewater on charcoal, kaolinite, and tafla, Desalination Water Treat., 56 (2015) 1536-1546.
[25] K.K. Choy, J.F. Porter, G. McKay, Langmuir isotherm models applied to the multicomponent sorption of acid dyes from effluent onto activated carbon, J. Chem. Eng. Data, 45 (2000) 575-584.
[26] B.E. Reed, M.R. Matsumoto, Modeling cadmium adsorption by activated carbon using the Langmuir and Freundlich isotherm expressions, Sep. Sci. Technol., 28 (1993) 2179-2195.
[27] G.P. Jeppu, T.P. Clement, A modified Langmuir-Freundlich isotherm model for simulating pH-dependent adsorption effects, J. Contam. Hydrol., 129 (2012) 46-53.
[28] S.V. Mohan, J. Karthikeyan, Removal of lignin and tannin colour from aqueous solution by adsorption onto activated charcoal, Environ. Pollut., 97 (1997) 183-187.
[29] Y. Bulut, Z. Tez, Adsorption studies on ground shells of hazelnut and almond, J. Hazard. Mater., 149 (2007) 35-41.
[30] L. Xiong, C. Chen, Q. Chen, J. Ni, Adsorption of Pb (II) and Cd (II) from aqueous solutions using titanate nanotubes prepared via hydrothermal method, J. Hazard. Mater., 189 (2011) 741-748.
[31] G. Akkaya, A. Özer, Biosorption of Acid Red 274 (AR 274) on Dicranella varia: Determination of equilibrium and kinetic model parameters, Process Biochem., 40 (2005) 3559-3568.
[32] J.V. Milojković, M.L. Mihajlović, M.D. Stojanović, Z.R. Lopičić, M.S. Petrović, T.D. Šoštarić, M.Đ. Ristić, Pb (II) removal from aqueous solution by Myriophyllum spicatum and its compost: equilibrium, kinetic and thermodynamic study, J. Chem. Technol. Biotechnol., 89 (2014) 662-670.
[33] E.A. Abdelrahman, R.M. Hegazey, R.E. El-Azabawy, Efficient removal of methylene blue dye from aqueous media using Fe/Si, Cr/Si, Ni/Si, and Zn/Si amorphous novel adsorbents, J. Mater. Res. Technol, 8 (2019) 5301-5313.